



OPEN

Solubility measurement and modeling of hydroxychloroquine sulfate (antimalarial medication) in supercritical carbon dioxide

Gholamhossein Sodeifian^{1,2,3}✉, Chandrasekhar Garlapati⁴, Maryam Arbab Nooshabadi⁵, Fariba Razmimanesh^{1,2,3} & Amirmuhammad Tabibzadeh^{1,2,3}

A supercritical fluid, such as supercritical carbon dioxide (scCO₂) is increasingly used for the micronization of pharmaceuticals in the recent past. The role of scCO₂ as a green solvent in supercritical fluid (SCF) process is decided by the solubility information of the pharmaceutical compound in scCO₂. The commonly used SCF processes are the rapid expansion of supercritical solution (RESS) and supercritical antisolvent precipitation (SAS). To implement micronization process, solubility of pharmaceuticals in scCO₂ is required. Present study is aimed at both measuring and modeling of solubilities of hydroxychloroquine sulfate (HCQS) in scCO₂. Experiments were conducted at various conditions (P = 12 to 27 MPa and T = 308 to 338 K), for the first time. The measured solubilities were found to be ranging between (0.0304 × 10⁻⁴ and 0.1459 × 10⁻⁴) at 308 K, (0.0627 × 10⁻⁴ and 0.3158 × 10⁻⁴) at 318 K, (0.0982 × 10⁻⁴ and 0.4351 × 10⁻⁴) at 328 K, (0.1398 × 10⁻⁴ and 0.5515 × 10⁻⁴) at 338 K. To expand the usage of the data, various models were tested. For the modelling task existing models (Chrastil, reformulated Chrastil, Méndez-Santiago and Teja (MST), Bartle et al., Reddy-Garlapati, Sodeifian et al., models) and new set of solvate complex models were considered. Among the all models investigated Reddy-Garlapati and new solvate complex models are able to fit the data with the least error. Finally, the total and solvation enthalpies of HCQS in scCO₂ were calculated with the help of model constants obtained from Chrastil, reformulated Chrastil and Bartle et al., models.

List of symbols

A_1, B_1	Constants of Eqs. (19) and (20)
A_2, B_2	Constants of Eq. (21)
A_3, B_3, C_3	Constants of Eq. (22)
A_4, B_4, C_4	Constants of Eq. (23)
$A_5, B_5, C_5, D_5, E_5, F_5$	Constants of Eq. (24)
$A_6, B_6, C_6, D_6, E_6, F_6$	Constants of Eq. (25)
AARD%	Average absolute relative deviation percentage
AIC	Akaike Information Criterion
AIC _c	Corrected AIC
C_s	Drug in sample in vial (g/L)
E1 to E14	Symbols used in experimental setup
H_{sol}	Solvation enthalpy (kJ/mol)
H_{sub}	Sublimation enthalpy (kJ/mol)

¹Department of Chemical Engineering, Faculty of Engineering, University of Kashan, Kashan 87317-53153, Iran. ²Laboratory of Supercritical Fluids and Nanotechnology, University of Kashan, Kashan 87317-53153, Iran. ³Modeling and Simulation Centre, Faculty of Engineering, University of Kashan, Kashan 87317-53153, Iran. ⁴Department of Chemical Engineering, Puducherry Technological University, Puducherry 605014, India. ⁵Bolvar Ghotbe Ravandi, Kashan Branch, Islamic Azad University, Ostaadan Street, Kashan 87159-98151, Iran. ✉email: sodeifian@kashanu.ac.ir

H_{total}	Total enthalpy (kJ/mol)
M_{CO_2}, M_S	Molar mass of CO_2 and drug (g/mol)
n_{CO_2}	Moles of carbon dioxide
n_{drug}	Moles of drug
N	Number of experimental data points
NIST	National Institute of Standards and Technology
OF	Objective function
Q	Number of parameters of a model
P	System pressure
P_c, P_r	Critical pressure, Reduced pressure
P_s	Sublimation pressure (Pa)
R	Universal constant of ideal gas, 8.314 J/mol K
RMSD	Root mean square deviation
S	Solubility (g/L)
SSE	Sum of squares error
sc CO_2	Supercritical carbon dioxide
T	System temperature (K)
T_c	Critical temperature (K)
v_1, v_2, v_s	Molar volume of solvent, solute and solute (m^3/mol)
V_l, V_s	Sampling loop and collection vial volumes (μL)
γ_2	Drug solute solubility in mole fraction

Greek symbols

α, α'	Constants in Eqs. (16) and (38), respectively
β, β'	Constants in Eqs. (16) and (38), respectively
ρ, ρ_r	Density, reduced density
$\kappa, \kappa', \kappa'', \kappa'''$	Association numbers
γ_2^∞	Infinitesimally dilute state activity coefficient of solute
$\lambda'_{12}, \lambda'_{21}$	Energies of interaction

There has been greater attention in the recent past about the application of supercritical carbon dioxide in micronization of pharmaceuticals^{1–5}. The drug administration is decided by the size of the particle. As we know, intravenous drug delivery requires particles size ranging from 0.1 to 0.3 μm , inhalation delivery requires 1–5 μm and oral delivery requires 0.1–100 μm and the smaller the size of the particles, greater chance of a drug being absorbed by the human body, which helps in reducing the drug dosage¹. Conventional particle reduction techniques result in products that are in the particulate range, for example jet mills provides product particles in the range 5–45 μm , hammer mill provides product particles in the range 25–600 μm , on the other hand supercritical fluids (SCFs) technology provides product particles in the range 0.1–600 μm ¹. But, to apply SCFs technology, solubility data of a specific drug in the desired SCF is required for the selection and design of suitable SCF process that reduces the particle size, thus the solubility will determine the operating condition of the process^{6–8}. Present work is focused on the both solubility measurement and modelling of hydroxychloroquine sulfate (HCQS) in sc CO_2 . This drug was originally developed in United States (US) to counter malaria in the year 1949^{9,10}. HCQS is considered as better alternate to chloroquine, due to less toxicity. It is also used for the treatment of Rheumatoid Arthritis (RA) and Systemic Lupus Erythematosus (SLE)^{9,11} disease. A recent study conducted by Pishnamazi et al., on the solubility of chloroquine in sc CO_2 has inspired us to take up this task¹². Since 1950, chloroquine has been in use to treat malaria, however, hydroxychloroquine, a chloroquine analogue has a better safety profile due to a hydroxyl group on the side chain and is used in the treatment of connective tissue disorders¹³. We believe this study helps to implement SCF technology to get the desired drug size particles of HCQS and which may help to reduce the drug dosage in treatment. To expand the use of solubility data, modelling is performed with literature models and new solvate complex models.

This work is carried out in two steps. In the first, HCQS solubility in sc CO_2 solvent is determined and in the second, data measured in the first stage are correlated with literature models. The models employed are solid–liquid equilibrium, Chrastil, reformulated Chrastil, Méndez-Santiago and Teja (MST), Bartle et al., Reddy-Garlapati, Sodeifian et al., models and three forms of new solvate complex models.

Experimental

Materials. HCQS was supplied by TEMAD Co., Active Pharmaceuticals in gradients, Mashhad, Iran (CAS Number: 747-36-4, mass purity > 99%). CO_2 (CAS Number: 124-38-9, mass purity > 99.9%) was purchased from Fadak company, Kashan, Iran. All the relevant details are tabulated in Table 1.

Solubility measurement details. SCF-solubility of the drugs was experimentally measured via two broad classes of saturated solution-based methods, where solubility measurement can be done either (1) statically or (2) dynamically¹⁴. In the present work, a UV–vis spectrophotometer was utilized to statically examine the equilibrium solubility data of HCQS in a setup presented in Fig. 1. This experimental setup has already been validated in our previous work with alpha-tocopherol and naphthalene¹⁵. The solubilities were measured with the help of an equilibrium cell. Thermodynamically, the method employed may be regarded as an isobaric–isothermal method¹⁴. All the measurements are taken by keeping system temperatures and pressures at the desired

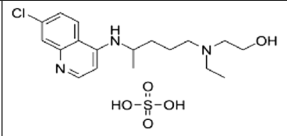
Compound	Formula	Structure	M_w (g/mol)	λ_{max} (nm)	CAS number	Minimum purity (%)
Hydroxychloroquine sulfate	$C_{18}H_{28}ClN_3O_5S$		434	220	747-36-4	99
Carbon dioxide	CO_2		44.01		124-38-9	99.9

Table 1. Molecular structure and physicochemical properties of used materials.

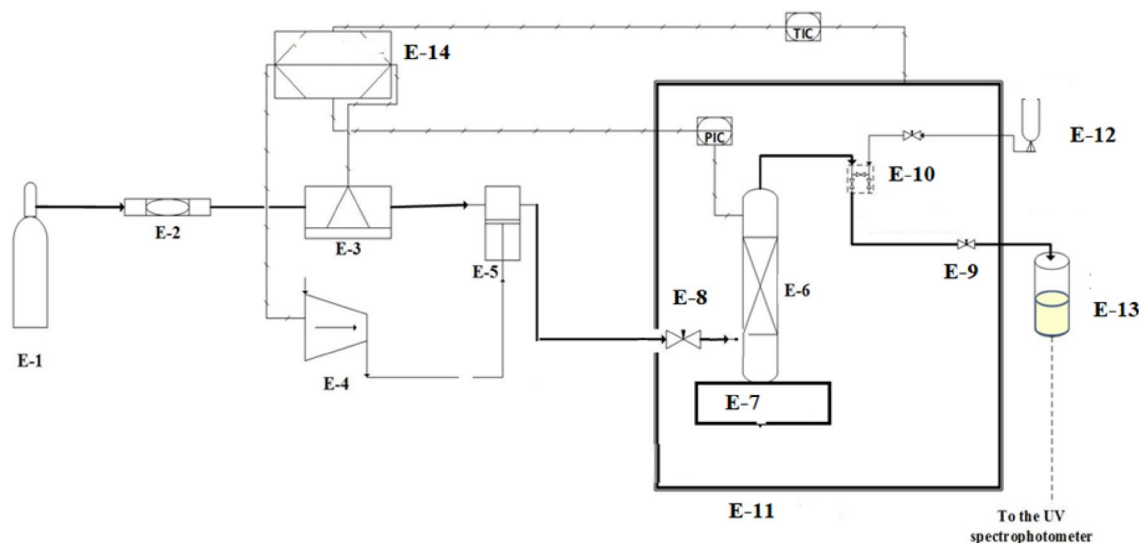


Figure 1. Experimental setup for solubility measurement, E1- CO_2 cylinder; E2- Filter; E3- Refrigerator unit; E4- Air compressor; E5- High pressure pump; E6- Equilibrium cell; E7- Magnetic stirrer; E8- Needle valve; E9- Back-pressure valve; E10- Six-port, two position valve; E11- Oven; E12- Syringe; E13- Collection vial; and E14- Control panel.

value with high precision (i.e., ± 0.1 K and ± 0.1 MPa). Complete details about the equipment and measurement procedures are presented elsewhere^{15–35}. However, the description of the equipment and the methodology employed in establishing solubility data are briefly presented in this section. The $scCO_2$ is pumped to the equilibrium cell and drug sample and $scCO_2$ are thoroughly mixed and allowed to attain equilibrium. It is observed that the equilibrium is attained in 60 min. To ensure equilibrium solubility, the experiments are performed with fresh samples at various time intervals. For a specified temperature and pressure in each experiment, the drug sample is contacted with $scCO_2$ and stirred thoroughly in an equilibrium cell until a specific time (5 min, 10 min, 20 min, 30 min, 40 min, 50 min and 60 min) and the solubility readings are recorded. It is observed that the solubility is independent of time after 30 min. However, for solubility measurement, the samples are collected after 1 h. For each sampling a 600 μ L volume saturated sample is collected via a collection valve in a deionized water preloaded sample vial. After discharging of each sample, the sampling valve was cleaned with 1 ml of deionized water. Drug sample solubility is estimated with the following formula:

$$y_2 = \frac{n_{drug}}{n_{drug} + n_{CO_2}} \quad (1)$$

where y_2 is solubility of the drug in $scCO_2$, n_{drug} and n_{CO_2} are number of moles of the drug and CO_2 in the sampling loop, respectively.

The following formulas are used in data conversion

$$n_{drug} = \frac{C_s \cdot V_s}{M_s} \quad (2)$$

$$n_{CO_2} = \frac{V_1 \rho_1}{M_{CO_2}} \quad (3)$$

where C_s is concentration of the drug in g/L. $V_1 = 600 \times 10^{-6}$ L and $V_s = 5 \times 10^{-3}$ L are sampling loop and vial volumes, respectively. M_s and M_{CO_2} are drug and CO_2 molecular weights, respectively. ρ_1 is density of $scCO_2$ at each experimental condition, as presented in Table 2.

Temperature (K) ^a	Pressure (bar) ^a	Density of scCO ₂ (kg/m ³) ⁵⁶	Mole fraction, y ₂ (×10 ⁵)	Experimental standard deviation, S(\bar{y})×10 ⁵	Equilibrium solubility, S (g/L)	Expanded uncertainty of mole fraction, U (×10 ⁵)
308	120	769	0.0304	0.001	0.0231	0.0024
	150	817	0.0434	0.0014	0.0350	0.0034
	180	849	0.0592	0.0021	0.0497	0.0048
	210	875	0.1087	0.0041	0.0939	0.0095
	240	896	0.1231	0.0051	0.1088	0.0115
	270	914	0.1459	0.0061	0.1316	0.0138
318	120	661	0.0627	0.0011	0.0409	0.0037
	150	744	0.1098	0.0021	0.0806	0.0065
	180	791	0.1406	0.0041	0.1097	0.0104
	210	824	0.2029	0.0065	0.1650	0.0158
	240	851	0.2498	0.0121	0.2097	0.0264
	270	872	0.3158	0.0073	0.2718	0.0202
328	120	509	0.0982	0.0012	0.0494	0.0049
	150	656	0.1591	0.0051	0.1029	0.0125
	180	725	0.1970	0.0091	0.1409	0.0202
	210	769	0.2731	0.0019	0.2072	0.0127
	240	802	0.3154	0.0121	0.2496	0.0279
	270	829	0.4351	0.0183	0.3557	0.0413
338	120	388	0.1398	0.0018	0.0534	0.0074
	150	557	0.2297	0.0021	0.1263	0.0117
	180	652	0.2822	0.0115	0.1816	0.0262
	210	710	0.3299	0.0098	0.2312	0.0245
	240	751	0.3921	0.0041	0.2906	0.0192
	270	783	0.5515	0.0065	0.4262	0.0275

Table 2. Solubility of HCQS in scCO₂ at various temperatures and pressures. y₂ and S are mole fraction of HCQS in scCO₂ and equilibrium solubility (g/L), respectively. The experimental standard deviation was

obtained by $S(y_k) = \sqrt{\frac{\sum_{j=1}^n (y_j - \bar{y})^2}{n-1}}$. Expanded uncertainty (U) and the relative combined standard uncertainty (u_{combined}/y) are defined, respectively, as follows: $(U) = k \cdot u_{\text{combined}}$ ($k=2$) and

$u_{\text{combined}}/y = \sqrt{\sum_{i=1}^N (P_i u(x_i)/x_i)^2}$. In this research, $u(x_i)$ was considered as standard uncertainties of

temperature, pressure, mole fraction, volumes and absorption. P_i , sensitivity coefficients, are equal to the partial derivatives of y equation (Eq. 1) with respect to the x_i . ^aStandard uncertainty values are $u(T) = \pm 0.1$ K and $u(p) = \pm 1$ bar. The value of the coverage factor $k=2$ was chosen on the basis of the level of confidence of approximately 95%.

Solubility is also described as

$$S = \frac{C_s V_s}{V_1} \quad (4)$$

The solubility and mole fraction relation is described as

$$S = \frac{\rho M_s}{M_{\text{CO}_2}} \frac{y_2}{1 - y_2} \quad (5)$$

The HCQS's solubility is quantified in the UV-Visible spectrophotometer (Model UNICO-4802) with the help of deionized water ($\text{conductivity} \leq 5 \mu\text{S m}^{-1}$) as collection solvent with the wave length of 220 nm at UV spectrum.

Modelling

Although there are several approaches in modelling solubility data, solid-gas equilibrium (known as equation of state (EoS) approach), solid-liquid equilibrium (SLE, also known as expanded liquid equilibrium approach) and empirical modelling are commonly used in literature for the data correlation³⁶⁻⁵⁰. For EoS approach critical properties of both solvent (scCO₂) and solute (HCQS) are required, whereas the SLE approach requires only melting temperature and melting enthalpy of the solute, but empirical modelling doesn't need any such information. HCQS is a typical compound and it is not possible to estimate its critical properties due to the presence of H₂SO₄ in its structure. Due to this fact EoS modelling is not persuaded. On the other hand, experimental

melting temperature and melting enthalpies of HCQS are available; due to this reason expanded liquid modelling is explored. For empirical modelling the density of scCO_2 , and system temperature and pressure are required; since they are readily available, it is also persuaded here. For empirical modelling, six commonly used solubility models are considered and those models have a varying number of parameters in their equations ranging from three to seven. The modelling purpose of some empirical models is to check the self-consistency of the measured data and to estimation some of the thermodynamic information of the dissolution process. In general, solubility of solids in SCFs is visualized in terms of solvate complex formation; therefore, a new set of solvate complex models is proposed for the better data fitting/correlation. More details about all the models considered in this work are presented in the following subsections.

Solid–liquid equilibrium (SLE) models. In this approach the HCQS solute is assumed to be infinitesimally dissolved in the scCO_2 solvent. At equilibrium, the drug fugacity in solid phase is equal to that of fugacity of drug in scCO_2 phase. From this criterion, the following solubility expression is proposed^{51–57}.

$$y_2 = \frac{1}{\gamma_2^\infty} \frac{f_2^S}{f_2^L} \quad (6)$$

From the literature, there are several models for this approach. However, Wilson activity coefficient model is considered for the data regression⁵⁸.

We know from thermodynamics, f_2^S/f_2^L ratio is

$$\frac{f_2^S}{f_2^L} = \exp \left[\frac{\Delta H_2^m}{RT} \left(\frac{T}{T_m} - 1 \right) - \int_{T_m}^T \frac{1}{RT^2} \left[\int_{T_m}^T [\Delta C_p] dT \right] dT \right] \quad (7)$$

Simplified expression for f_2^S/f_2^L is²⁷

$$\ln \left(\frac{f_2^S}{f_2^L} \right) = \frac{\Delta H_2^m}{RT} \left(\frac{T}{T_m} - 1 \right) \quad (8)$$

The required γ_2^∞ is obtained from Wilson model and the relevant expressions are as follows:

$$\ln(\gamma_2^\infty) = 1 - \Lambda_{12} - \ln(\Lambda_{21}) \quad (9)$$

where

$$\Lambda_{12} = \frac{v_2}{v_1} \exp \left(-\frac{\lambda_{12}}{RT} \right) \quad (10)$$

$$\Lambda_{21} = \frac{v_1}{v_2} \exp \left(-\frac{\lambda_{21}}{RT} \right) \quad (11)$$

$$\Lambda_{12} = v_2 \rho_{c1} \rho_r \exp \left(-\frac{\lambda'_{12}}{T_r} \right) \quad (12)$$

$$\Lambda_{12} = \frac{1}{v_2 \rho_{c1} \rho_r} \exp \left(-\frac{\lambda'_{21}}{T_r} \right) \quad (13)$$

$$\lambda'_{12} = \frac{\lambda_{12}}{RT_{c1}} \text{ and } \lambda'_{21} = \frac{\lambda_{21}}{RT_{c1}}$$

$$\ln v_2 (\text{m}^3 \text{mol}^{-1}) = \alpha_2 \ln \rho_1 (\text{kg m}^{-3}) + \beta_2 \quad (14)$$

$$v_2 = \alpha \rho_r + \beta \quad (15)$$

On combining Eqs. (10)–(15), we get

$$\Lambda_{12} = (\alpha \rho_r + \beta) \rho_{c1} \rho_r \exp \left(-\frac{\lambda'_{12}}{T_r} \right) \quad (16)$$

$$\Lambda_{21} = \frac{1}{(\alpha\rho_r + \beta)\rho_{c1}\rho_r} \exp\left(-\frac{\lambda'_{21}}{T_r}\right) \quad (17)$$

λ'_{21} and λ'_{12} are the energies of interactions, where subscripts 1 and 2 denote solvent and solute, respectively. Combining all the equations, finally, resulted in SLE model, i.e., Eq. (18)

$$y_2 = \exp\left(\frac{\Delta H_2^m}{RT}\left(\frac{T}{T_m} - 1\right)\right) / \exp\left(1 - (\alpha\rho_r + \beta)\rho_{c1}\rho_r \exp\left(-\frac{\lambda'_{12}}{T_r}\right) - \ln\left(\frac{1}{(\alpha\rho_r + \beta)\rho_{c1}\rho_r} \exp\left(-\frac{\lambda'_{21}}{T_r}\right)\right)\right) \quad (18)$$

Commonly used empirical models. *Chrastil's model*⁵⁹. In the year 1981, Josef Chrastil presented a model for the solubility of solids/liquids in SCF. The main basis of the model is a solvate complex formulation based on a simple reaction. According to Chrastil, solubility is explained by $c_2 = c_2(\kappa, \rho_1, T)$, where κ is association number, ρ_1 is solvent density (scCO₂) and T is temperature. Chrastil proposed Eq. (19)

$$c_2 = \rho_1^\kappa \exp\left(A_1 + \frac{B_1}{T}\right) \quad (19)$$

An alternative from of Eq. (19) is Eq. (20)⁶⁰

$$y_2 = \frac{(\rho_1)^{\kappa-1} \exp\left(A_1 + \frac{B_1}{T}\right)}{\left[1 + (\rho_1)^{\kappa-1} \exp\left(A_1 + \frac{B_1}{T}\right)\right]} \quad (20)$$

where y_2 is solute solubility in mole fraction.

*Reformulated Chrastil's model*⁶¹. In the year 2009, Garlpati and Madras has reformulated Chrastil's model and it is expressed by Eq. (21), where solubility is explained by $y_2 = y_2(\kappa', \rho_1, T)$, in which κ' is association number, ρ_1 is solvent density (scCO₂) and T is temperature.

$$y_2 = \left(\frac{RT\rho_1}{M_{ScF}f^*}\right)^{\kappa'-1} \exp\left(A_2 + \frac{B_2}{T}\right) \quad (21)$$

in Eq. (21), R denotes universal constant of ideal gas, M_{ScF} is molecular weight of solvent, f^* is reference pressure and A_2 and B_2 are the Reformulated model constants.

*Méndez-Santiago and Teja (MST) model*⁶². The MST model is used to check the consistency of the data. All the data falls around a single straight line when $T \ln(y_2P) - C_3T$ versus ρ_1 is established. MST model is expressed as Eq. (22)

$$T \ln(y_2P) = A_3 + B_3\rho_1 + C_3T \quad (22)$$

where A_3 to C_3 are the model constants.

*Bartle et al., model*⁶³. The solute sublimation enthalpy is calculated with Bartle et al., model and it is stated as

$$\ln\left(\frac{y_2P}{P_{ref}}\right) = A_4 + \frac{B_4}{T} + C_4(\rho_1 - \rho_{ref}) \quad (23)$$

where A_4 to C_4 are the model constants. Using the constant B_4 , sublimation enthalpy is calculated (i.e., $\Delta_{sub}H = -B_4R$).

*Reddy-Garlapati model*⁶⁴. It is the model developed based on the degree of freedom analysis based on drug compounds. According to this model, solubility, $y_2 = y_2(T_r, P_r)$, is expressed as Eq. (24), where T_r and P_r are reduced temperature and pressures, respectively.

$$y_2 = (A_5 + B_5P_r + C_5P_r^2)T_r + (D_5 + E_5P_r + F_5P_r^2) \quad (24)$$

where A_5 to F_5 are the model constants.

*Sodeifian et al., model*⁶⁵. It is another recently proposed empirical model. According to this model, solubility, $y_2 = y_2(T, P, \rho_1)$, can be calculated by

$$y_2 = A_6 + B_6\frac{P^2}{T} + C_6 \ln(\rho_1T) + D_6\rho_1 \ln(\rho_1) + E_6P \ln(T) + F_6\frac{\ln(\rho_1)}{T} \quad (25)$$

where A_6 to F_6 are the model constants.

New solvate complex models⁶⁶. The solubility is visualized via solvate complex formation. The following simple reversible reaction is considered for the formation of solvate complex AB_κ , in which 'A' is designated as solute and the letter 'B' is designated as solvent in SCF mixture.



At equilibrium

$$K_f = \frac{\left(\hat{f}_{AB_\kappa} / f_{AB_\kappa}^*\right)_{SP}}{\left(\hat{f}_A / f_A^*\right)_{Solid} \left(\hat{f}_B / f_B^*\right)_{SP}^\kappa} \quad (27)$$

where the subscript 'Solid' is designated as solid phase and subscript 'SP' is designated as solvent phase and superscript '*' is reference state.

For each species the fugacity's expressions are

$$\hat{f}_A = y_A \hat{\phi}_A P \quad (28)$$

$$\hat{f}_B = y_B \hat{\phi}_B P \quad (29)$$

$$\hat{f}_{AB_\kappa} = y_{AB_\kappa} \hat{\phi}_{AB_\kappa} P \quad (30)$$

$$f_{AB_\kappa}^* = \phi_{AB_\kappa}^* P^* \quad (31)$$

$$f_A^* = \phi_A^* P^* \quad (32)$$

$$f_B^* = \phi_B^* P^* \quad (33)$$

At equilibrium in vapour phase only two things exist: one is solvent and the other is solvate complex thus

$$y_B + y_{AB_\kappa} = 1 \quad (34)$$

where y_B, y_{AB_κ} are respective mole fractions.

If we assume the standard state of species 'A' is pure under same system conditions. Then

$$\hat{f}_A = f_A \quad (35)$$

Fugacity of species 'A' can be written as

$$f_A = P_A^{Sub} \exp \left[\frac{v_A (P - P_A^{Sub})}{RT} \right] \quad (36)$$

From thermodynamics, equilibrium constant is function of salvation enthalpy as Eq. (37)

$$\ln (K_f) = \Delta H_s / RT + q_s \quad (37)$$

Sublimation pressure can be expressed as Eq. (38)

$$\ln (P_A^{Sub}) = \alpha' - \beta' / T \quad (38)$$

Substituting Eqs. (35)–(38) into Eq. (27) along with two simplifications gives Eq. (39)

One assumption that $v_A P / RT$ is expressed as $Z v_A \rho_1 / M$ where ρ_1 is the density of the supercritical phase and the second assumption is referred to negligible term $v_A P_A^{Sub} / RT (\sim 10^{-8} - 10^{-9})$ [since the sublimation pressures are very low and their order is about $(\sim 10^{-3} - 10^{-4})$ and the drug molar volume is also about the order $(\sim 10^{-4})$]^{67–70}.

$$\ln (y_{AB_\kappa}) - \kappa \ln (y_B) + (1 - \kappa'') \ln (P / P^*) = L / T + M \rho + N \quad (39)$$

where $L = (\Delta H_s / R - \beta')$, $M = (-Z v_A / M)$ and $N = \ln \left(\frac{(\phi_A^*) (\hat{\phi}_{AB_\kappa} / \phi_{AB_\kappa}^*)}{(\hat{\phi}_B / \phi_B^*)^\kappa} \right) + \ln P^* + q_s - \alpha'$

Equation (39) is rearranged as Eq. (40)

$$y_{AB_\kappa} = (y_B)^{\kappa''} (P / P^*)^{(\kappa'' - 1)} \exp (L / T + M \rho + N) \quad (40)$$

Further, on rearranging Eq. (40), we get Eq. (41)

$$y_{AB_\kappa} / (1 - y_{AB_\kappa})^{\kappa''} = (P / P^*)^{(\kappa'' - 1)} \exp (L / T + M \rho + N) \quad (41)$$

Applying binomial expansion to the left side term gives Eq. (41)

$$y_{AB\kappa} / (1 - \kappa'' y_{AB\kappa}) = (P/P^*)^{(\kappa''-1)} \exp(L/T + M\rho + N) \quad (42)$$

We know solubility, y_2 , is related to cluster mole fraction $y_{AB\kappa}$ as Eq. (43)^{68,69}

$$y_2 = y_{AB\kappa} / (1 + \kappa'' y_{AB\kappa}) \quad (43)$$

Thus the solubility is expressed as Eq. (44)

$$y_2 = (P/P^*)^{(\kappa''-1)} \exp(L/T + M\rho + N) / \left[1 + \kappa'' \left[(P/P^*)^{(\kappa''-1)} \exp(L/T + M\rho + N) \right] \right] \quad (44)$$

κ'' is a function of reduced density, given by Eq. (45)⁷¹

$$\kappa'' = a_1 + a_2\rho_r + a_3\rho_r^2 \quad (45)$$

Combining Eqs. (44) and (45) results in Eq. (46)

$$y_2 = (P/P^*)^{(a_1+a_2\rho_r+a_3\rho_r^2-1)} \exp(L/T + M\rho + N) / \left[1 + (a_1 + a_2\rho_r + a_3\rho_r^2) \left[(P/P^*)^{(a_1+a_2\rho_r+a_3\rho_r^2-1)} \exp(L/T + M\rho + N) \right] \right] \quad (46)$$

To reduce the number constants in Eq. (46), we have a choice to choose κ as a linear function of reduced density or as constant. Thus, we get the following two reduced solubility expressions.

$$y_2 = (P/P^*)^{(a_1+a_2\rho_r-1)} \exp(L/T + M\rho + N) / \left[1 + (a_1 + a_2\rho_r) \left[(P/P^*)^{(a_1+a_2\rho_r-1)} \exp(L/T + M\rho + N) \right] \right] \quad (47)$$

and

$$y_2 = (P/P^*)^{(\kappa''-1)} \exp(L/T + M\rho + N) / \left[1 + (\kappa'') \left[(P/P^*)^{(\kappa''-1)} \exp(L/T + M\rho + N) \right] \right] \quad (48)$$

In literature, related solubility expression is proposed by Rajasekhar and Madras⁶⁷ as

$$y_2 = \left(\frac{P}{P^*} \right)^{(\kappa'''-1)} \exp(L'/T + M'\rho + N') \quad (49)$$

The correlating abilities and evaluation of the new models (Eqs. 46–48) and existing model (Eq. 49) are also carried out in this work.

The data fitting to the models are performed by an objective function Eq. (50)⁷²

$$OF = \sum_{i=1}^N \frac{|y_{2i}^{\text{exp}} - y_{2i}^{\text{calc}}|}{y_{2i}^{\text{exp}}} \quad (50)$$

The obtained deviations are indicated in terms of an average absolute relative deviation percentage (AARD%).

$$\text{AARD\%} = \left(100/N_i \right) \sum_{i=1}^N \frac{|y_{2i}^{\text{exp}} - y_{2i}^{\text{calc}}|}{y_{2i}^{\text{exp}}} \quad (51)$$

The entire regression task was done using (MATLAB 2019a*) version software, also this can be performed by nonlinear regression methods with the same results^{84,85}.

Results and discussion

The experimental device used for the measurement of HCQS solubility in scCO₂ is accurate and reliable. It was successfully tested to reproduce the solubilities of naphthalene in scCO₂ and alpha-tocopherol in scCO₂ systems and the same was reported in our earlier work¹⁵. The solubility values reported for alpha-tocopherol in our previous work, are the average of three replicate measurements with relative standard deviations lower than 5.7%¹⁵. The solubility values of naphthalene reported in our previous work are also the average of three replicate measurements with relative standard deviations lower than 6.5%¹⁵. Table 2 shows the measured solubilities of HCQS in scCO₂ at various conditions and the density of the scCO₂, obtained from the NIST data base⁷³. From solubility data, it is clear that present system (HCQS+scCO₂), does not exhibit the usual retrograde phenomenon. Affecting solvent density and solute power, the temperature was found to impose a dual impact on solubility in scCO₂ depending on how the solute vapor pressure and solvent density are balanced. In this respect, increasing the solution temperature may enhance the solute vapor pressure, thereby contributing to stronger solvating power of SCE. At the same time, a rise of temperature may lower the scCO₂ density which is known to depreciate the overall solvating power of the fluid. The mole fraction versus pressure isotherms on Fig. 2 suggest an enhancement in the solubility of drug upon elevating the temperature. This proves the dominant role of the solute vapor pressure in determining the solubility behavior irrespective of the pressure. Reports by other researchers confirm the results of the present work regarding the effect of temperature on the solubility in scCO₂^{74–76}. From Table 2 and Fig. 2, it is clear that when temperature is raised from 308 to 338 K, there is a clear indication of a rise in solubility from 0.0304×10^{-4} to 0.1398×10^{-4} at 12 MPa (i.e., 4.6 folds' increase) and at 27 MPa from

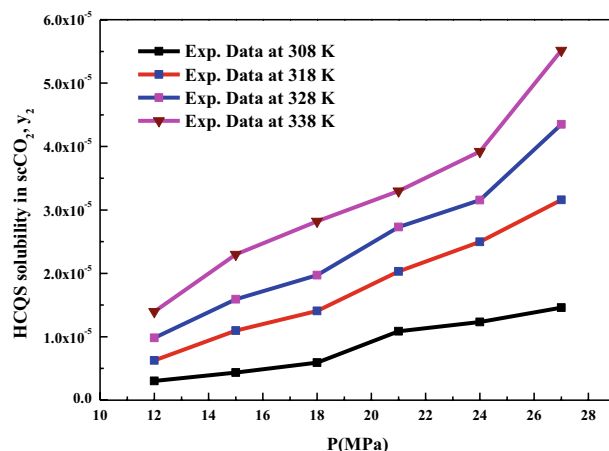


Figure 2. Solubility isotherms of HCQS in scCO₂.

0.1459×10^{-4} to 0.5515×10^{-4} (i.e., 3.8 folds increase). At the same time, at 12 MPa, the density of scCO₂ changes from 769 to 338 kg m⁻³ at 308 and 338 K, respectively. Similarly, the density of scCO₂ at 27 MPa changes from 914 to 783 kg m⁻³ at 308 and 338 K, respectively; which means that there is decrease in density at 12 MPa (low pressure) (i.e., $338/769 = 0.4395$) and there is increase in density to some extent at 27 MPa (higher pressure) (i.e., $783/914 = 0.8567$). Thus, the solubility behavior of HCQS in scCO₂ is highly nonlinear. This kind of high nonlinearity behavior has been observed with amlodipine besylate-scCO₂ in the recent past²⁸. This kind of high nonlinearity behavior can't be captured with simple models. Thus models having more adjustable constants are required to fit the data and this would augment the justification for the need of development of new models.

All the regression results are summarized in Table 3 and presented in Figs. 3, 4, 5, 6, 7, 8 and 9. Solid-liquid model requires enthalpy of fusion, molar volume and melting point of the solute. Enthalpy of fusion is estimated with the help Jain et al.⁷⁷, and molar volume of the solute is estimated with the help Immirzi and Perini method⁷⁸. The calculated molar enthalpy and molar volumes are 65,208 J mol⁻¹ and 3.306×10^{-4} m³ mol⁻¹, respectively. The melting temperature is obtained from the material safety data sheet as 240 °C. From Chrastil's model constant (B_1), total enthalpy is calculated ($B_1 \times R$). From Bartle's model constant (B_4), sublimation enthalpy is calculated ($\Delta_{sub}H = -B_4R$). From the magnitude difference between total and sublimation enthalpies, solvation enthalpy is calculated. Similarly, from reformulated Chrastil's model constant (B_2) and Bartle's model constant (B_4), combination solvation enthalpy is calculated. All the calculated quantities are shown in Table 4. The regression

Model	Correlation parameters	AARD%	R ²	R ² _{adj}
Solid-liquid equilibrium (SLE)	$\alpha = 4.9285 \times 10^{-3}; \beta = -1.156 \times 10^{-3};$ $\lambda'_{12} = 0.43761; \lambda'_{21} = 3.0828$	17.27	0.927	0.912
Chrastil	$\kappa = 3.8918; A_1 = -4.2291; B_1 = -8391.6$	24.27	0.829	0.804
Reformulated Chrastil	$\kappa' = 3.8833; A_2 = -18.92; B_2 = -7457.9$	24.32	0.828	0.803
Méndez-Santiago and Teja (MST)	$A_3 = -12,530; B_3 = 2.2133; C_3 = 25.435$	26.50	0.779	0.769
Bartle	$A_4 = 26.917; B_4 = -10,711; C_4 = 6.8092 \times 10^{-3}$	27.04	0.787	0.777
Reddy-Garlapati	$A_5 = 1.04535 \times 10^{-4}; B_5 = -2.179 \times 10^{-5};$ $C_5 = 1.897 \times 10^{-5}; D_5 = -1.4246 \times 10^{-4}$ $E_5 = 1.7054 \times 10^{-5}; F_5 = -1.684 \times 10^{-5}$	10.04	0.974	0.973
Sodeifan	$A_6 = 8.6490; B_6 = -1.0492 \times 10^{-3};$ $C_6 = 3.0286 \times 10^{-1}; D_6 = 7.1397 \times 10^{-4}$ $E_6 = 1.9898 \times 10^{-2}; F_6 = -4.9173 \times 10^2$	13.10	0.944	0.941
Solvate complex-Eq. (46)	$\kappa'' = a_1 + a_2\rho_r + a_3\rho_r^2$ where $a_1 = 0.58597; a_2 = 2.6675$ $a_3 = -0.40881$ and $L = -2207.3$ $M = -0.018958; N = -4.6158$ $\kappa''_{ave} = 3.78$	10.08	0.96	0.958
Solvate complex-Eq. (47)	$\kappa'' = a_1 + a_2\rho_r$ where $a_1 = -0.28155; a_2 = 1.5579$ and $L = -6206.5; M = -0.015134; N = 13.107$ $\kappa''_{ave} = 2.21$	12.00	0.955	0.951
Solvate complex- Eq. (48)	$\kappa = 3.089; L = -4162; M = -8.4529 \times 10^{-4};$ $N = -8.4428$	12.30	0.949	0.941
Rajasekhar and Madras-Eq. (49)	$\kappa''' = 3.089; L' = -4162; M' = -8.4529 \times 10^{-4};$ $N' = -8.4428$	12.30	0.949	0.9411

Table 3. Regression results of all models used in this research.

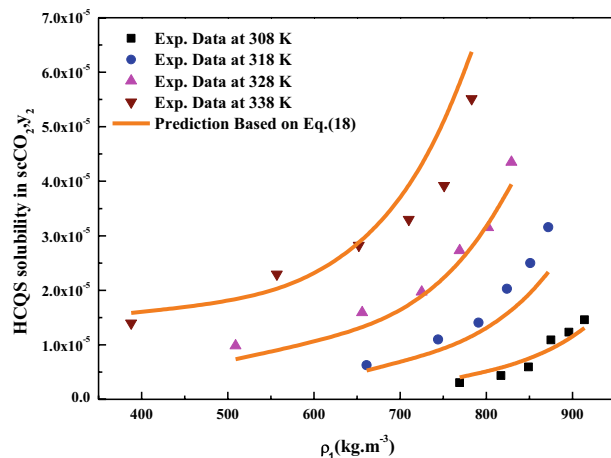


Figure 3. HCQS solubility in scCO₂ versus ρ_1 . Symbols are experimental data points. Solid lines are calculated from SLE model (Eq. 18).

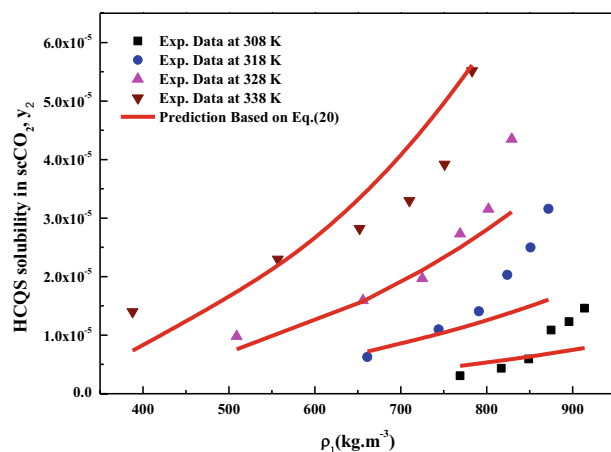


Figure 4. HCQS solubility in scCO₂ versus ρ_1 . Symbols are experimental data points. Solid lines are calculated from Chrastil's model (Eq. 20).

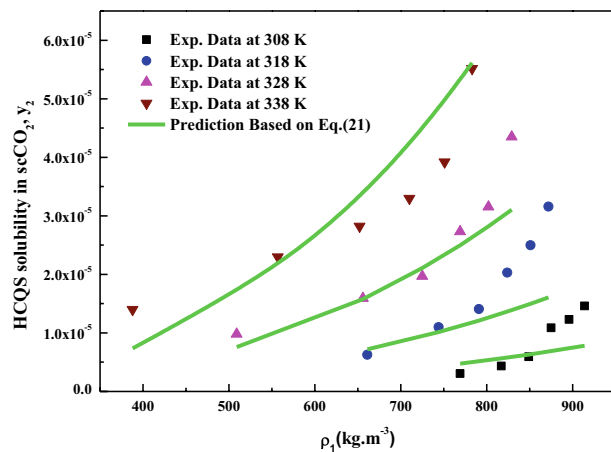


Figure 5. HCQS solubility in scCO₂ versus ρ_1 . Symbols are experimental data points. Solid lines are calculated from SLE model (Eq. 21).

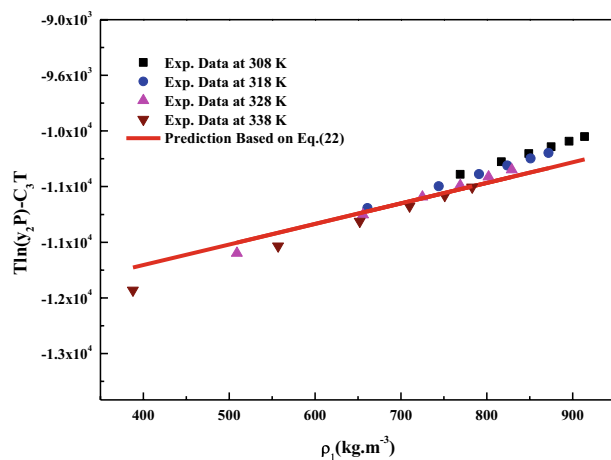


Figure 6. Self-consistency plot based on MST model (Eq. 22).

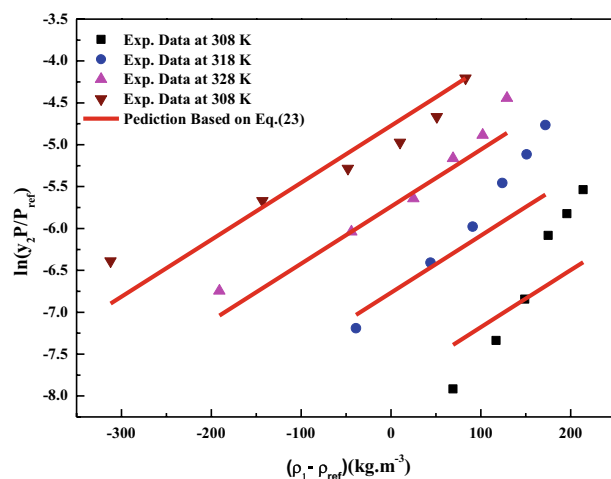


Figure 7. $\ln(y_2 P/P_{ref})$ versus $(\rho_1 - \rho_{ref})$. Symbols are experimental data points. Solid lines are calculated from Bartle et al., model (Eq. 23).

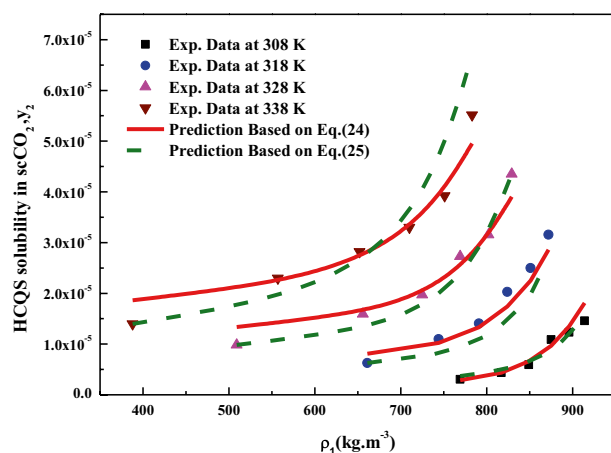


Figure 8. HCQS solubility in $scCO_2$ versus ρ_1 . Symbols are experimental data points. Solid lines and broken lines are calculated from Reddy-Garlapati and Sodeifian models (Eqs. 24, 25), respectively.

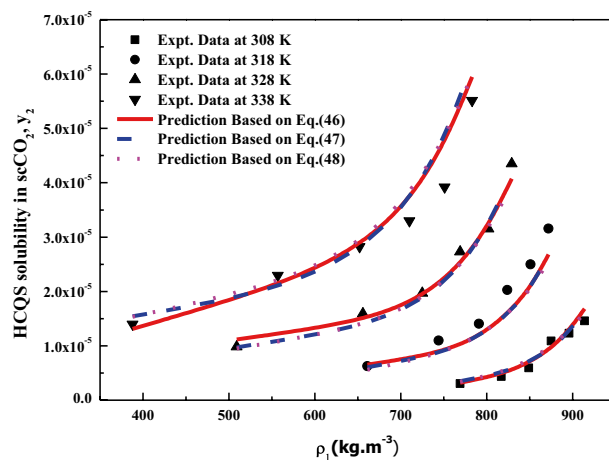


Figure 9. HCQS solubility in scCO_2 versus ρ_1 . Symbols and lines are experimental and calculated from new solvate complex models (Eqs. 46, 47, 48), respectively.

ability of commonly used three parameter models are found to be inferior when compared to Sodeifian et al., and Reddy–Garlapati models. This may be due to a smaller number of parameters in the models; on the other hand, the correlating ability of the solvate complex models is quite good. However, among all empirical models, Reddy–Garlapati model is the best model. The newly proposed solvate complex models have more adjustable constants, and thus their predictions are also good. From the solvate complex model's constants, it is interesting to note the behavior of association number. When association number is treated as a linear function of reduced density, the obtained average association number for the solubility data is $\kappa''_{ave} = 2.21$, which is lesser than that of the conventional Chrastil's model $\kappa = 3.89$. But, when association number is treated as quadratic function of reduced density, the obtained average association number for the solubility data is $\kappa''_{ave} = 3.78$, and it is matching well with association number of Chrastil's model. From those results and from literature arguments, we can infer that association number is quadratic function of ρ_r so that is apparent than other forms and its correlations are reliable^{71,79}. Thus, association number as quadratic function of ρ_r is recommended for the data interpolation.

Further, a comparative analysis is done to determine the best model for HCQS- scCO_2 system. Since, a varying number of parameters are involved in the equations considered in the work, Akaike Information Criterion (AIC) and corrected AIC (AIC_c)^{80–83} are used to identify the best model. AIC alone is used when data points are more than forty; on the other hand, AIC_c is used when data points are less than forty. In the present there are only twenty-four solubility data points in our hands; hence, AIC_c is used for identifying the best model. AIC_c is defined as Eq. (52)

$$\text{AIC}_c = \text{AIC} + \frac{2Q(Q+1)}{N-Q-1} \quad (52)$$

where N is solubility data points, Q is number of model constants, and SSE is error sum of squares. From the least AIC_c value, the best model is identified. The lower the AIC_c value the greater the accuracy of the model, and it is independent of the number of parameter. All the AIC_c values are reported in Table 5. From results, Reddy–Garlapati and the new solvate complex models are observed to be the better models.

Conclusion

Solubilities of solid HCQS in scCO_2 solvent were measured at various conditions ranging from $P = 12$ to 27 MPa and $T = 308$ to 338 K. The measured data's range is from 0.0304×10^{-4} to 0.5515×10^{-4} in terms of mole fraction. Three forms of solvate complex models explored in this study are reasonable in estimating solubility and among the three the best model is observed to have AIC_c and AARD values -595.4 and 10.08% respectively. Among

Model	Name of property		
	Total Enthalpy, ΔH_{total} (kJ/mol)	Enthalpy of sublimation ΔH_{sub} (kJ/mol)	Enthalpy of solvation (kJ/mol)
Chrastil's model	69.80 ^a		-19.30^d
Modified Chrastil's model	62.00 ^b		-27.10^e
Bartle et al., model		89.1 ^c (approximate value)	

Table 4. Enthalpies of sublimation and solvation of HCQS. ^dObtained as a result of difference between ΔH_{sub}^c and $\Delta H_{\text{total}}^a$. ^eObtained as a result of difference between ΔH_{sub}^c and $\Delta H_{\text{total}}^b$.

Model	SSE ($\cdot 10^{10}$)	RMSE ($\cdot 10^6$)	N	Q	AIC	AIC _c
Standard solubility models						
Chrastil's model	9.284	6.219	3	24	-569.4	-568.2
Modified Chrastil's model	9.349	6.241	3	24	-569.2	-568.0
Mendez-Teja model	6.935	5.375	3	24	-500.1	-498.4
Bartle et al., model	11.923	7.048	5	24	-563.4	-562.2
Reddy-Garlapati model	1.381	2.399	6	24	-609.1	-604.1
Sodeifian et al., model	3.956	4.060	6	24	-583.9	-579.7
Solvate complex models						
Equation (46)	1.99	14.124	6	24	-600.0	-595.4
Equation (47)	2.54	15.925	5	24	-597.0	-593.2
Equation (48)	2.55	15.961	4	24	-598.0	-596.3
Equation (49)	2.55	15.961	4	24	-598.0	-596.3

Table 5. Summary of SSE, RMSE, AIC and AIC_c of all solubility models.

empirical models Reddy-Garlapati model is observed to fit the data quite well and with the corresponding AIC_c and AARD values -604.1 and 10.04%, respectively.

Data availability

On request the data may be obtained from the corresponding author.

Received: 4 February 2023; Accepted: 9 May 2023

Published online: 19 May 2023

References

1. Taberner, A., del Valle, E. M. M. & Galán, M. A. Supercritical fluids for pharmaceutical particle engineering: Methods, basic fundamentals and modelling. *Chem. Eng. Process* **60**, 9–25. <https://doi.org/10.1016/j.cep.2012.06.004> (2012).
2. Subramaniam, B., Rajewski, R. A. & Snavely, K. Pharmaceutical processing with supercritical carbon dioxide. *J. Pharm. Sci.* **86**(8), 885–890. <https://doi.org/10.1021/js9700661> (1997).
3. Elvassore, N. K. I. Pharmaceutical processing with supercritical fluids. In *High Pressure Process Technology: Fundamentals and Applications* (ed. Bertucco, A. G. V. G.) 612–625 (Elsevier Science, 2001).
4. Gupta, R. B., Chattopadhyay, P. Method of forming nanoparticles and microparticles of controllable size using supercritical fluids and ultrasound. US patent No. 20020000681 (2002).
5. Reverchon, E., Adami, R., Caputo, G. & De Marco, I. Spherical microparticles production by supercritical antisolvent precipitation: Interpretation of results. *J. Supercrit. Fluids* **47**(1), 70–84. <https://doi.org/10.1016/j.supflu.2008.06.002> (2008).
6. Sodeifian, G., Ardestani, N. S., Sajadian, S. A. & Panah, H. S. Experimental measurements and thermodynamic modeling of Coumarin-7 solid solubility in supercritical carbon dioxide: Production of nanoparticles via RESS method. *Fluid Phase Equilib.* **483**, 122–143. <https://doi.org/10.1016/j.fluid.2018.11.006> (2019).
7. Sodeifian, G., Sajadian, S. A., Ardestani, N. S. & Razmimanesh, F. Production of loratadine drug nanoparticles using ultrasonic-assisted rapid expansion of supercritical solution into aqueous solution (US-RESSAS). *J. Supercrit. Fluids* **147**, 241–253. <https://doi.org/10.1016/j.fluid.2018.05.018> (2019).
8. Mukhopadhyay, M. Partial molar volume reduction of solvent for solute crystallization using carbon dioxide as antisolvent. *J. Supercrit. Fluids* **25**(3), 213–223. [https://doi.org/10.1016/S0896-8446\(02\)00147-X](https://doi.org/10.1016/S0896-8446(02)00147-X) (2003).
9. Dongala, T. et al. In vitro different biological pH conditions of hydroxychloroquine sulfate tablets is available for the treatment of COVID-19. *Front. Mol. Biosci.* **7**, 613393. <https://doi.org/10.3389/fmolb.2020.613393> (2021).
10. de Margerie, V. et al. Continuous manufacture of hydroxychloroquine sulfate drug products via hot melt extrusion technology to meet increased demand during a global pandemic: From bench to pilot scale. *Int. J. Pharm.* **605**, 120818. <https://doi.org/10.1016/j.ijpharm.2021.120818> (2021).
11. Bodur, S., Erarpat, S., Günkara, O. T. & Bakırdere, S. Accurate and sensitive determination of hydroxychloroquine sulfate used on COVID-19 patients in human urine, serum and saliva samples by GC-MS. *J. Pharm. Anal.* **11**(3), 278–283. <https://doi.org/10.1016/j.jpha.2021.01.006> (2021).
12. Pishnamazi, M. et al. Chloroquine (antimalaria medication with anti SARS-CoV activity) solubility in supercritical carbon dioxide. *J. Mol. Liq.* **322**, 114539. <https://doi.org/10.1016/j.molliq.2020.114539> (2021).
13. Doyno, C., Sobieraj, D. M. & Baker, W. Toxicity of chloroquine and hydroxychloroquine following therapeutic use or overdose. *Clin. Toxicol.* **59**(1), 12–23. <https://doi.org/10.1080/15563650.2020.1817479> (2020).
14. Peper, S., Fonseca, J. M. & Dohrn, R. High-pressure fluid-phase equilibria: Trends, recent developments, and systems investigated (2009–2012). *Fluid Phase Equilib.* **484**, 126–224. <https://doi.org/10.1016/J.FLUID.2018.10.007> (2019).
15. Sodeifian, G., Sajadian, S. A. & Ardestani, N. S. Determination of solubility of Aprepitant (an antiemetic drug for chemotherapy) in supercritical carbon dioxide: Empirical and thermodynamic models. *J. Supercrit. Fluids* **128**, 102–111. <https://doi.org/10.1016/j.supflu.2017.05.019> (2017).
16. Sodeifian, G., Razmimanesh, F., Sajadian, S. A. & Hazaveie, S. M. Experimental data and thermodynamic modeling of solubility of Sorafenib tosylate, as an anti-cancer drug, in supercritical carbon dioxide: Evaluation of Wong–Sandler mixing rule. *J. Chem. Thermodyn.* **142**, 105998. <https://doi.org/10.1016/j.jct.2019.105998> (2020).
17. Sodeifian, G., Razmimanesh, F. & Sajadian, S. A. Prediction of solubility of sunitinib malate (an anti-cancer drug) in supercritical carbon dioxide (SC-CO₂): Experimental correlations and thermodynamic modeling. *J. Mol. Liq.* **297**, 111740. <https://doi.org/10.1016/j.molliq.2019.111740> (2020).
18. Sodeifian, G. & Sajadian, S. A. Solubility measurement and preparation of nanoparticles of an anticancer drug (Letrozole) using rapid expansion of supercritical solutions with solid cosolvent (RESS-SC). *J. Supercrit. Fluids* **133**(1), 239–252. <https://doi.org/10.1016/j.supflu.2017.10.015> (2018).

19. Sodeifian, G., Razmimanesh, F., Ardestani, N. S. & Sajadian, S. A. Experimental data and thermodynamic modeling of solubility of Azathioprine, as an immunosuppressive and anti-cancer drug, in supercritical carbon dioxide. *J. Mol. Liq.* **299**, 112179. <https://doi.org/10.1016/j.molliq.2019.112179> (2019).
20. Hazaveie, S. M., Sodeifian, G. & Sajadian, S. A. Measurement and thermodynamic modeling of solubility of Tamsulosin drug (anti cancer and anti-prostatic tumor activity) in supercritical carbon dioxide. *J. Supercrit. Fluids* **163**, 104875. <https://doi.org/10.1016/j.supflu.2020.104875> (2020).
21. Sodeifian, G., Alwi, R. S., Razmimanesh, F. & Roshanghias, A. Solubility of pazopanib hydrochloride (PZH, anticancer drug) in supercritical CO₂: Experimental and thermodynamic modeling. *J. Supercrit. Fluids* **190**, 105759. <https://doi.org/10.1016/j.supflu.2022.105759> (2022).
22. Sodeifian, G., Alwi, R. S., Razmimanesh, F. & Abadian, M. Solubility of Dasatinib monohydrate (anticancer drug) in supercritical CO₂: Experimental and thermodynamic modeling. *J. Mol. Liq.* **346**, 117899. <https://doi.org/10.1016/j.molliq.2021.117899> (2022).
23. Sodeifian, G., Alwi, R. S., Razmimanesh, F. & Tamura, K. Solubility of quetiapine hemifumarate (antipsychotic drug) in supercritical carbon dioxide: Experimental, modeling and hansen solubility parameter application. *Fluid Phase Equilib.* **537**, 113003. <https://doi.org/10.1016/j.fluid.2021.113003> (2021).
24. Sodeifian, G., Garlapati, C., Razmimanesh, F. & Ghanaat-Ghamsari, M. Measurement and modeling of clemastine fumarate (antihistamine drug) solubility in supercritical carbon dioxide. *Sci. Rep.* **11**(1), 1–16. <https://doi.org/10.1038/s41598-021-03596-y> (2021).
25. Sodeifian, G., Nasri, L., Razmimanesh, F. & Abadian, M. CO₂ utilization for determining solubility of teriflunomide (immunomodulatory agent) in supercritical carbon dioxide: Experimental investigation and thermodynamic modeling. *J. CO₂ Util.* **58**, 101931. <https://doi.org/10.1016/j.jcou.2022.101931> (2022).
26. Sodeifian, G., Ardestani, N. S., Sajadian, S. A. & Panah, H. S. Measurement, correlation and thermodynamic modeling of the solubility of Ketotifen fumarate (KTF) in supercritical carbon dioxide: Evaluation of PCP-SAFT equation of state. *J. Fluid Phase Equilib.* **458**, 102–114. <https://doi.org/10.1016/j.fluid.2017.11.016> (2018).
27. Sodeifian, G., Detakhsheshpour, R. & Sajadian, S. A. Experimental study and thermodynamic modeling of Esomeprazole (proton-pump inhibitor drug for stomach acid reduction) solubility in supercritical carbon dioxide. *J. Supercrit. Fluids* **154**, 104606. <https://doi.org/10.1016/j.supflu.2019.104606> (2019).
28. Sodeifian, G., Garlapati, C., Razmimanesh, F. & Sodeifian, F. Solubility of amlodipine besylate (calcium channel blocker drug) in supercritical carbon dioxide: Measurement and correlations. *J. Chem. Eng. Data.* **66**(2), 1119–1131. <https://doi.org/10.1021/acs.jced.0c00913> (2021).
29. Sodeifian, G., Garlapati, C., Razmimanesh, F. & Sodeifian, F. The solubility of Sulfabenzamide (an antibacterial drug) in supercritical carbon dioxide: Evaluation of a new thermodynamic model. *J. Mol. Liq.* **335**, 116446. <https://doi.org/10.1016/j.molliq.2021.116446> (2021).
30. Sodeifian, G., Hazaveie, S. M., Sajadian, S. A. & Saadati Ardestani, N. Determination of the solubility of the repaglinide drug in supercritical carbon dioxide: Experimental data and thermodynamic modeling. *J. Chem. Eng. Data* **64**(12), 5338–5348. <https://doi.org/10.1021/acs.jced.9b00550> (2019).
31. Sodeifian, G., Hsieh, C.-M., Derakhsheshpour, R., Chen, Y.-M. & Razmimanesh, F. Measurement and modeling of metoclopramide hydrochloride (anti-emetic drug) solubility in supercritical carbon dioxide. *Arab. J. Chem.* <https://doi.org/10.1016/j.arabjc.2022.103876> (2022).
32. Sodeifian, G., Nasri, L., Razmimanesh, F. & Abadian, M. Measuring and modeling the solubility of an antihypertensive drug (losartan potassium, Cozaar) in supercritical carbon dioxide. *J. Mol. Liq.* **331**, 115745. <https://doi.org/10.1016/j.molliq.2021.115745> (2021).
33. Sodeifian, G., Razmimanesh, F., Sajadian, S. A. & Panah, H. S. Solubility measurement of an antihistamine drug (Loratadine) in supercritical carbon dioxide: Assessment of qCPA and PCP-SAFT equations of state. *Fluid Phase Equilib.* **472**, 147–159. <https://doi.org/10.1016/j.fluid.2018.05.018> (2018).
34. Sodeifian, G., Sajadian, S. A. & Razmimanesh, F. Solubility of an antiarrhythmic drug (amiodarone hydrochloride) in supercritical carbon dioxide: Experimental and modeling. *Fluid Phase Equilib.* **450**, 149–159. <https://doi.org/10.1016/j.fluid.2017.07.015> (2017).
35. Sodeifian, G., Sajadian, S. A., Razmimanesh, F. & Hazaveie, S. M. Solubility of Ketoconazole (antifungal drug) in SC-CO₂ for binary and ternary systems: Measurements and empirical correlations. *Sci. Rep.* **11**(1), 1–13. <https://doi.org/10.1038/s41598-021-87243-6> (2021).
36. Sodeifian, G., Alwi, R. S. & Razmimanesh, F. Solubility of *Pholcodine* (antitussive drug) in supercritical carbon dioxide: Experimental data and thermodynamic modeling. *J. Fluid Phase Equilib.* **566**, 113396. <https://doi.org/10.1016/j.fluid.2022.113396> (2022).
37. Sodeifian, G., Garlapati, C., Razmimanesh, F. & Nateghi, H. Solubility measurement and thermodynamic modeling of pantoprazole sodium sesquihydrate in supercritical carbon dioxide. *Sci. Rep.* **12**, 7758. <https://doi.org/10.1038/s41598-022-11887-1> (2022).
38. Sodeifian, G., Hazaveie, S. M. & Sodeifian, F. Determination of Galantamine solubility (an anti alzheimer drug) in supercritical carbon dioxide (CO₂): Experimental correlation and thermodynamic modeling. *J. Mol. Liq.* **330**, 115695. <https://doi.org/10.1016/j.molliq.2021.115695> (2021).
39. Sodeifian, G., Ardestani, N. S., Razmimanesh, F. & Sajadian, S. A. Experimental and thermodynamic analysis of supercritical CO₂-solubility of minoxidil as an antihypertensive drug. *Fluid Phase Equilib.* **522**, 112745. <https://doi.org/10.1016/j.fluid.2020.112745> (2020).
40. Sodeifian, G., Garlapati, C., Hazaveie, S. M. & Sodeifian, F. Solubility of 2,4,7-triamino-6-phenylpteridine (triamterene, diuretic drug) in supercritical carbon dioxide: Experimental data and modeling. *J. Chem. Eng. Data* **65**(9), 4406–4416. <https://doi.org/10.1021/acs.jced.0c00268> (2020).
41. Sodeifian, G., Ardestani, N. S., Sajadian, S. A., Golmohammadi, M. R. & Fazlali, A. Solubility of sodium valproate in supercritical carbon dioxide: Experimental study and thermodynamic modeling. *J. Chem. Eng. Data* **65**(4), 1747–1760. <https://doi.org/10.1021/acs.jced.9b01069> (2020).
42. Sodeifian, G., Sajadian, S. A. & Derakhsheshpour, R. Experimental measurement and thermodynamic modeling of Lansoprazole solubility in supercritical carbon dioxide: Application of SAFT-VR EoS. *Fluid Phase Equilib.* **507**, 112422. <https://doi.org/10.1016/j.fluid.2019.112422> (2020).
43. Sodeifian, G., Hazaveie, S. M., Sajadian, S. A. & Razmimanesh, F. Experimental investigation and modeling of the solubility of oxcabazepine (an anti convulsant agent) in supercritical carbon dioxide. *Fluid Phase Equilib.* **493**, 160–173. <https://doi.org/10.1016/j.fluid.2019.04.013> (2019).
44. Sodeifian, G. & Sajadian, S. A. Experimental measurement of solubilities of sertraline hydrochloride in supercritical carbon dioxide with/without menthol: Data correlation. *J. Supercrit. Fluids* **149**, 79–87. <https://doi.org/10.1016/j.supflu.2019.03.020> (2019).
45. Sodeifian, G., Usefi, M. M. B., Razmimanesh, F. & Roshanghias, A. Determination of the solubility of rivaroxaban (anticoagulant drug, for the treatment and prevention of blood clotting) in supercritical carbon dioxide: Experimental data correlations. *Arab. J. Chem.* **16**(1), 104421. <https://doi.org/10.1016/j.arabjc.2022.104421> (2023).
46. Abadian, M., Sodeifian, G., Razmimanesh, F. & Mahmoudabadi, S. Z. Experimental measurement and thermodynamic modeling of solubility of Riluzole drug (neuroprotective agent) in supercritical carbon dioxide. *Fluid Phase Equilib.* **567**, 113711. <https://doi.org/10.1016/j.fluid.2022.113711> (2023).
47. Sodeifian, G., Garlapati, C. & Roshanghias, A. Experimental solubility and modelling of crizotinib (anti cancer medication) in supercritical carbon dioxide. *Sci. Rep.* **12**, 17494. <https://doi.org/10.1038/s41598-022-22366-y> (2022).

48. Sodeifian, G., Alwi, R. S., Razmimanesh, F. & Sodeifian, F. Solubility of prazosin hydrochloride (alpha blocker antihypertensive drug) in supercritical CO₂: Experimental and thermodynamic modeling. *J Mol Liq* **362**, 119689. <https://doi.org/10.1016/j.molliq.2022.119689> (2022).
49. Sodeifian, G., Nasri, L., Razmimanesh, F. & Nooshabadi, M. A. Solubility of ibuprofen in supercritical carbon dioxide (Sc-CO₂): Data correlation and thermodynamic analysis. *J. Chem. Thermodyn.* **182**, 107050. <https://doi.org/10.1016/j.jct.2023.107050> (2023).
50. Sodeifian, G., Hsieh, C.-M., Tabibzadeh, A., Wang, H.-C. & Nooshabadi, M. A. solubility of palbociclib in supercritical carbon dioxide from experimental measurement and Peng–Robinson equation of state. *Sci. Rep.* **13**, 2172. <https://doi.org/10.1038/s41598-023-29228-1> (2023).
51. Mahesh, G. & Garlapati, C. Modelling of solubility of some parabens in supercritical carbon dioxide and new correlations. *Arab. J. Sci. Eng.* <https://doi.org/10.1007/s13369-021-05500-2> (2021).
52. Alwi, R. S. & Tamura, K. Measurement and correlation of derivatized anthraquinone solubility in supercritical carbon dioxide. *J. Chem. Eng. Data* **60**(10), 3046–3052. <https://doi.org/10.1021/acs.jced.5b00480> (2015).
53. Alwi, R. S., Tanaka, T. & Tamura, K. Measurement and correlation of solubility of anthraquinone dyestuffs in supercritical carbon dioxide. *J. Chem. Thermodyn.* **74**, 119–125. <https://doi.org/10.1016/j.jct.2014.01.015> (2014).
54. Kramer, A. & Thodos, G. Solubility of 1-hexadecanol and palmitic acid in supercritical carbon dioxide. *J. Chem. Eng. Data* **33**, 230–234. <https://doi.org/10.1021/je00053a002> (1988).
55. Iwai, Y., Koga, Y., Fukuda, T. & Arai, Y. Correlation of solubilities of high boiling components in supercritical carbon dioxide using a solution model. *J. Chem. Eng. Jpn.* **25**, 757–760. <https://doi.org/10.1252/jcej.25.757> (1992).
56. Alwi, R. S., Garlapati, C. & Tamura, K. Solubility of anthraquinone derivatives in supercritical carbon dioxide: New correlations. *Molecules* **26**(2), 460. <https://doi.org/10.3390/molecules26020460> (2021).
57. Kramer, A. & Tdodos, G. Adaptation of the Flory–Huggins theory for modeling supercritical solubilities of solids. *Ind. Eng. Chem. Res.* **27**, 1506–1510. <https://doi.org/10.1021/ie00080a026> (1988).
58. Nasri, L., Benseititi, Z. & Bensaad, S. Modeling of the solubility in supercritical carbon dioxide of some solid solute isomers using the expanded liquid theory. *J. Sci. Technol.* **3**(2), 39–44 (2018).
59. Chrastil, J. Solubility of solids and liquids in supercritical gases. *J. Phys. Chem.* **86**(15), 3016–3021. <https://doi.org/10.1021/j100212a041> (1982).
60. Sridar, R., Bhowal, A. & Garlapati, C. A new model for the solubility of dye compounds in supercritical carbon dioxide. *Thermochim. Acta* **561**, 91–97. <https://doi.org/10.1016/j.tca.2013.03.029> (2013).
61. Garlapati, C. & Madras, G. Solubilities of palmitic and stearic fatty acids in supercritical carbon dioxide. *J. Chem. Thermodyn.* **42**(2), 193–197. <https://doi.org/10.1016/j.jct.2009.08.001> (2010).
62. Méndez-Santiago, J. & Teja, A. S. The solubility of solids in supercritical fluids. *Fluid Phase Equilib.* **158**, 501–510. [https://doi.org/10.1016/S0378-3812\(99\)00154-5](https://doi.org/10.1016/S0378-3812(99)00154-5) (1999).
63. Bartle, K. D., Clifford, A., Jafar, S. & Shilstone, G. Solubilities of solids and liquids of low volatility in supercritical carbon dioxide. *J. Phys. Chem. Ref. Data* **20**(4), 713–756. <https://doi.org/10.1063/1.555893> (1991).
64. Reddy, T. A. & Garlapati, C. Dimensionless empirical model to correlate pharmaceutical compound solubility in supercritical carbon dioxide. *Chem. Eng. Technol.* **42**(12), 2621–2630. <https://doi.org/10.1002/ceat.201900283> (2019).
65. Sodeifian, G., Razmimanesh, F. & Sajadian, S. A. Solubility measurement of a chemotherapeutic agent (Imatinib mesylate) in supercritical carbon dioxide: Assessment of new empirical model. *J. Supercrit. Fluids* **146**, 89–99. <https://doi.org/10.1016/j.supflu.2019.01.006> (2019).
66. Anita, N. & Garlapati, C. A simple model to correlate solubility of thermolabile solids in supercritical fluids. *AIP Conf. Proc.* **2446**, 180002. <https://doi.org/10.1063/5.0108042> (2022).
67. Rajasekhar, Ch. & Madras, G. An association model for the solubilities of pharmaceuticals in supercritical carbon dioxide. *Thermochim. Acta* **507–508**, 99–105. <https://doi.org/10.1016/j.tca.2010.05.006> (2010).
68. Li, Q., Zhong, C., Zhang, Z., Liu, Y. & Zhou, Q. An equilibrium model for the correlation of the solubility of solids in supercritical fluids with cosolvent. *Sep. Sci. Technol.* **38**, 1705–1719. <https://doi.org/10.1081/SS-120019404> (2003).
69. Sodeifian, G., Garlapati, C., Razmimanesh, F. & Nateghi, H. Experimental solubility and thermodynamic modeling of empagliflozin in supercritical carbon dioxide. *Sci. Rep.* **12**, 9008. <https://doi.org/10.1038/s41598-022-12769-2> (2022).
70. Reddy, S. N. & Madras, G. An association and Wilson activity coefficient model for solubilities of aromatic solid pollutants in supercritical carbon dioxide. *Thermochim. Acta* **541**, 49–56. <https://doi.org/10.1002/ceat.201900283> (2012).
71. Spark, D. L., Hernandez, R. & Estevez, L. A. Evaluation of density-based models for the solubility of solids in supercritical carbon dioxide and formulation of a new model. *Chem. Eng. Sci.* **63**, 4292–4301. <https://doi.org/10.1016/j.ces.2008.05.031> (2008).
72. Valderrama, J. O. & Alvarez, V. H. Correct way of representing results when modelling supercritical phase equilibria using equation of state. *Can. J. Chem. Eng.* **83**(3), 578–581. <https://doi.org/10.1002/cjce.5450830323> (2008).
73. National Institute of Standards and Technology U.S. Department of commerce, NIST Chemistry WebBook in 2018 October. <https://webbook.nist.gov/chemistry/> (05 December 2022).
74. Montequi, I., Alonso, E., Martín, A. & Cocero, M. J. Solubility of diisopropoxitanium bis (acetylacetonate) in supercritical carbon dioxide. *J. Chem. Eng. Data* **53**, 204–206. <https://doi.org/10.1021/je700503c> (2007).
75. Reddy, S. N. & Madras, G. Solubilities of benzene derivatives in supercritical carbon dioxide. *J. Chem. Eng. Data* **56**, 1695–1699. <https://doi.org/10.1021/je100863p> (2011).
76. Wang, H., Sang, J., Guo, L., Zhu, J. & Jin, J. Solubility of polyacrylamide in supercritical carbon dioxide. *J. Chem. Eng. Data* **62**, 341–347. <https://doi.org/10.1021/acs.jced.6b00677> (2016).
77. Jain, A., Yang, G. & Yalkowsky, S. H. Estimation of melting points of organic compounds. *Ind. Eng. Chem. Res.* **43**, 7618–7621. <https://doi.org/10.1021/ie049378m> (2004).
78. Immirzi, A. & Perini, B. Prediction of density in organic crystals. *Acta Crystall. A Crystallogr.* **33**, 216–218. <https://doi.org/10.1107/S0567739477000448> (1977).
79. Adachi, Y. & Lu, B. C.-Y. Supercritical fluid extraction with carbon dioxide and ethylene. *Fluid Phase Equilib.* **14**, 147–156. [https://doi.org/10.1016/0378-3812\(83\)80120-4](https://doi.org/10.1016/0378-3812(83)80120-4) (1983).
80. Akaike, H. Information theory and an extension of the maximum likelihood principle. In *Proceedings of the Second International Symposium on Information Theory* (ed. Petrov, B. N. C. F.) 267–281 (Akademai Kiado, 1973).
81. Burnham, K. P. & Anderson, D. R. Multimodel inference: Understanding AIC and BIC in model selection. *Sociol. Methods Res.* **33**(2), 261–304. <https://doi.org/10.1177/0049124104268644> (2004).
82. Kletting, P. & Glatting, G. Model selection for time-activity curves: The corrected Akaike information criterion and the F-test. *Z. Med. Phys.* **19**(3), 200–206. <https://doi.org/10.1016/j.zemedi.2009.05.003> (2009).
83. Anita, N. & Garlapati, C. A statistical analysis of solubility models employed in supercritical carbon dioxide. *AIP Conf. Proc.* **2446**, 180003. <https://doi.org/10.1063/5.0108200> (2022).
84. Haghtalab, A. & Sodeifian, G. Determination of the discrete relaxation spectrum for polybutadiene and polystyrene by a non-linear regression method. *Iran. Polym. J.* **11**, 107–113 (2002).
85. Sodeifian, G. & Haghtalab, A. Discrete relaxation spectrum and K-BKZ constitutive equation for PVC, NBR and their blends. *Appl. Rheol.* **14**, 180–189. <https://doi.org/10.1515/arh-2004-0010> (2004).

Acknowledgements

We wish to record our gratitude to University of Kashan (Grant # Pajoothaneh-1401/24) for the financial support.

Author contributions

G.S. Conceptualization, Methodology, Validation, Investigation, Supervision, Project administration, Writing-review and editing; C.G. Methodology, Investigation, Software, Writing-original draft; M.A.N. Validation, Measurement, Resources; F.R. Investigation, Validation. A.T. Measurement.

Competing interests

The authors declare no competing interests.

Additional information

Correspondence and requests for materials should be addressed to G.S.

Reprints and permissions information is available at www.nature.com/reprints.

Publisher's note Springer Nature remains neutral with regard to jurisdictional claims in published maps and institutional affiliations.



Open Access This article is licensed under a Creative Commons Attribution 4.0 International License, which permits use, sharing, adaptation, distribution and reproduction in any medium or format, as long as you give appropriate credit to the original author(s) and the source, provide a link to the Creative Commons licence, and indicate if changes were made. The images or other third party material in this article are included in the article's Creative Commons licence, unless indicated otherwise in a credit line to the material. If material is not included in the article's Creative Commons licence and your intended use is not permitted by statutory regulation or exceeds the permitted use, you will need to obtain permission directly from the copyright holder. To view a copy of this licence, visit <http://creativecommons.org/licenses/by/4.0/>.

© The Author(s) 2023